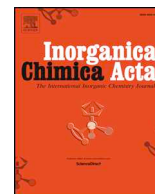




ELSEVIER

Contents lists available at ScienceDirect

Inorganica Chimica Acta

journal homepage: www.elsevier.com/locate/ica

Research paper

Resolution of ferrocene and deuterated ferrocene conformations using dynamic vibrational spectroscopy: Experiment and theory

R.M. Trevorah^a, N.T.T. Tran^a, D.R.T. Appadoo^b, F. Wang^c, C.T. Chantler^{a,*}^a School of Physics, University of Melbourne, Parkville, Vic 3010, Australia^b Australian Synchrotron, 800 Blackburn Rd., Clayton, Vic 3168, Australia^c Department of Chemistry and Biotechnology, Swinburne University of Technology, Hawthorn, Victoria 3122, Australia

ARTICLE INFO

Keywords:

IR

Stereochemical analysis

Ferrocene

High-resolution FTIR

ABSTRACT

The signature of molecular vibrations and distortions in dynamic molecules gives a complex fingerprint which is insightful and can substantiate (or otherwise) chemical hypotheses regarding molecular and conformer stability. Using high-accuracy experimental data of ferrocene (Fc) and deuterated ferrocene (dFc, $Fc - d^{10}$) at temperatures from 7 K through to 388 K, we obtain complex spectral profiles which require an advanced reaction coordinate model to explain. We obtain compelling evidence that the single conformer model (staggered D_{5d} or eclipsed D_{5h}) used to interpret and explain many experimental results on ferrocene is invalid. However we also present compelling evidence that mixed conformer models are invalid, where ferrocene is represented by an effective dihedral angle between the cyclopentadienyl (Cp) rings; or by a mixture of Boltzmann populations of the two conformers. We find no evidence for single or mixed conformer models despite covering almost all conclusions from past literature for gas, solution or solid phase Fc. Some molecular dynamics computations have imputed free rotation at liquid helium temperatures or at room temperature – we find no evidence for either of these hypotheses.

We measure and derive point-wise experimental uncertainty of the spectra, enabling quantitative assessment of specific chemical and physical models about the origin of the spectral line-shapes. A new principle based on the reaction coordinate is introduced. Advanced spectroscopy and modelling is introduced for hypothesis testing, to articulate the nature of the potential surface, the reaction coordinate and subtle conformational changes in dilute systems. Two expected spectral peaks appear inverted in the gas phase, but are explained by our Reaction Coordinate Method (RCM) model. The non-uniform broadening of the singlet and doublet peaks with increasing temperature is explained. Our experimental analysis shows that the lowest energy conformer is D_{5h} for both Fc and dFc. We are able to represent the reduced mass ratios of the lowest vibrational modes for Fc and dFc of 1.11 for ν_1 for Fc to and of 1.10 for Fc to $Fc - d^{10}$. The measured barrier height for rotation is 7.4 kJ mol^{-1} and 6.3 kJ mol^{-1} for Fc and dFc respectively, in comparison to numerous theoretical treatments and past experimental studies. For the first time, we obtain agreement of the model with the complex spectral evolution of profiles. These new techniques are sensitive discriminants of alternate models and chemical systems, which argues for wider application to other complex or impenetrable problems across fields arising for numerous other solutions, frozen or at room temperature.

1. Motivation

Ferrocene (Fc, $[Fe(C_5H_5)_2]$) is the iconic molecule of organometallic chemistry, where the ferrous sandwich structure exemplifies metal-aryl bonding, yet is also one of the most subtle. A serendipitous discovery of Fc more than sixty years ago, reported by two groups in late 1951 [4] and early 1952 [5], ultimately proved to be a breakthrough introducing a new era of organometallic chemistry. Wilkinson and coworkers proposed the structure of Fc to be a *sandwich compound* (a metal atom sandwiched between two cyclopentadienyl rings), possessing a

symmetry point group of D_{5d} (staggered) [6]. Independently, Fischer and co-workers proposed an iron (II) atom to be confined between staggered cyclopentadienyl (Cp) rings in the ferrocene molecule [7]. Subsequent X-ray crystallography studies [8–10] confirmed the sandwich form of the structure. A recent Nature Chemistry commentary [11] explained that key papers were insightful and generational without providing high standards of analysis.

New development of the understanding of ferrocene is of very broad interest and significance as it relates to the nature of the organometallic bond and advanced quantum chemistry. Fc, extended structures and

* Corresponding author.

E-mail address: chantler@unimelb.edu.au (C.T. Chantler).<https://doi.org/10.1016/j.ica.2020.119491>

Received 23 November 2019; Received in revised form 30 January 2020; Accepted 31 January 2020

Available online 17 February 2020

0020-1693/ Crown Copyright © 2020 Published by Elsevier B.V. All rights reserved.

analogous compounds have been adopted for various applications in catalysis [12], fuel additives and pharmaceuticals [13–16], and have been the subject of much structural investigation. In particular, the stability of these compounds and their catalytic activity are proposed to be highly dependent on their local electronic structures and conformation.

Ferrocene has two limiting conformations, D_{5h} and D_{5d} , depending on the relative orientation of the Cp rings (Fig. S9). Studies of deuterated ferrocene, dFc, provide analogous yet distinct insight into the dynamics of the Cp rings. Although long accepted that both Fc and dFc possess dual pentagonal carbon rings with a staggered conformation [6,7,17–20], angular separation between the Cp rings for crystalline Fc has been reported to vary at different temperatures: $22 \pm 2^\circ$ or $22(2)^\circ$ at 173 K; $28(2)^\circ$ at 298 K [21], 9.9° , 9.2° , 8.9° at temperatures of 148 K, 123 K, and 101 K respectively [22] (Table S3). Alternate experimental techniques have suggested stability of eclipsed or D_{5h} symmetry with a barrier height from almost zero [23] to $4\text{--}23 \text{ kJ mol}^{-1}$ using NMR, ADPs, QENS, XRD and electron scattering [24–26,22,27,28,23].

Theoretical studies for Fc suggest an eclipsed or D_{5h} symmetry should be more or less stable by up to 6 kJ mol^{-1} [29,30]. Such an alternate conformer has not been verified experimentally in a robust definitive manner, though some evidence has been presented using XAFS [31,32]. Density functional theory demonstrates that the predicted and observed torsional and swing vibrations of ferrocene are emblematic of layered, stacked, Cp rings rather than individual bonds [33–36]. Detailed studies of D_{5h} and D_{5d} of ferrocene are important as ferrocene derivatives inherit particular properties which only exist in one conformer. [37]. Table S5 summarises the previous experimental data of IR spectra of Fc in the $400\text{--}500 \text{ cm}^{-1}$ region. Band frequencies are presented in terms of two band profiles instead of three as the doublet is almost degenerate. The measured gas-phase IR spectra of Fc [18] shows inconsistency in terms of energy shifts (ca. 7 cm^{-1}) and frequency splitting (3 cm^{-1}) when compared with theory [2]. The IR band of Fc from monoclinic crystals claims a frequency splitting of 14 cm^{-1} [38], whilst the orthorhombic crystal claims a frequency splitting of 19 cm^{-1} . The IR spectra from the amorphous solid [39] and orthorhombic crystal provide the same band frequencies, and the band frequencies with the triclinic Fc crystal and with the Nujol solvent [17] appear consistent. Calculations by Gryaznova et al. [34] are significantly discrepant in terms of energy-shift, intensity and frequency splitting with other theory [2] and IR measurements [39,38]. The only measured gas-phase IR spectra [18] of dFc also disagrees with theoretical values [34,2] and raises major issues because of the apparent discrepancies.

The first IR measurements of the vibrational spectra of Fc were conducted by Lippincott and coworkers [17,18] more than 60 years ago. They concluded that the conformer was staggered, D_{5d} , but perhaps the key evidence must arise from the profile shape and asymmetry, as we consider in this work. The Fc doublet band in the IR spectrum appears to be weaker than the singlet in the vapour, and reversed in solution [18]. Hence it appears to be inverted in theoretical predictions. One of the features (around 675 cm^{-1}) in the Fc vapour spectra of Lippincott et al. [18] is not predicted from theory and may originate from experimental impurities, solvation or thermal effects (Supplementary information Fig. S10). Recent advances in *ab initio* calculations of molecular structure are now extremely useful for characterizing the Fc conformation in experimental data. Key clues can be obtained from deuterated Fc (dFc) measurements under cognate conditions. Detailed understanding of the rotation dynamics of the Cp rings requires a temperature series of measurements, because any Cp ring rotation is highly temperature dependent [1].

Earlier survey work [1,2] represented a dramatic milestone in the understanding of this complex dynamic quantum system, yet the estimates had sufficiently large discrepancies across the temperature range that possible conclusions invoked 30% population of off-axis rocking modes; large anharmonicity with increasing temperature; and differences in the calculated wavenumbers and intensities of the modes. In

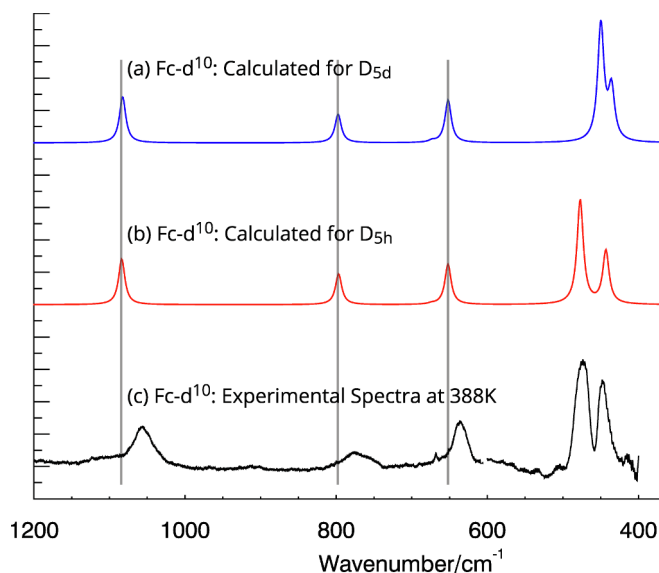


Fig. 1. Overview of spectral data and comparison of the qualitative accuracy of DFT computations across the IR spectral region for dFc, arguing for the good convergence and accuracy of the theoretical computations for this analysis. The full IR spectral region contains one additional peak at 3257 cm^{-1} . Vertical lines indicate typical offset of theoretical prediction from experiment. Most importantly, the new theory is able to distinguish the signatures of the key conformations in the critical spectral region. However, the spectral profile below 500 cm^{-1} is complex and challenging.

principle, and quantitatively, these are now resolved. The measurement of robust uncertainty permitted the beginning of advanced analysis and experiment [3].

2. Profile variation from theory between the conformers

The conformers are remarkably similar and IR, XAFS and XRD experimental data are almost identical, with little ability to discriminate between the D_{5h} and D_{5d} conformations. Fortunately, recent advanced DFT computation [2] has predicted a significant splitting of the IR spectrum according to conformation and thereby enabled a critical probe of the conformation. IR spectra of Fc were calculated by our group for the D_{5h} and D_{5d} conformations in gas-phase in a broad spectral region ($400\text{--}3500 \text{ cm}^{-1}$): six major peaks are apparent in the region for both conformers (Fig. 1) [2]. Except for a small separation of ‘singlet’ and ‘doublet’ transitions of circa 17 cm^{-1} in the $<500 \text{ cm}^{-1}$ region, the IR spectra of the conformers are practically identical. However, the band profiles in the $450\text{--}500 \text{ cm}^{-1}$ region are quite distinct between the D_{5h} and D_{5d} conformations and provide a key signature to distinguish between the conformations in experiment (Fig. S11). Except for our theoretical calculations [2], the available reported computations do not provide separated bands for the doubly degenerate peak in the $400\text{--}500 \text{ cm}^{-1}$ region.

The stereochemistry of Fc due to the relative orientation of the Cp rings can be understood in terms of two normal modes (Tables S4 and S5): a singlet (ν_7 , an A_2' mode due to the Fe atom oscillation between the rings) and a spectroscopic doublet ($\nu_{8,9}$, two E' modes due to the in-phase tilting of rings), in the $450\text{--}500 \text{ cm}^{-1}$ region. Whilst the relative intensity of the band due to the ‘doublet’ is predicted to be two times larger than the band for the singlet, the corresponding band frequency $\nu_{8,9}$ due to the doublet is calculated to be much larger for the D_{5h} form than the D_{5d} , and the band frequency ν_7 for the singlet is conversely larger for the D_{5d} form. The relative intensities and frequencies of the bands therefore provide a means of identifying the stereochemistry of Fc. There are a number of high quality DFT calculations [34,18] for ferrocene IR spectra (Table S6). Our recent theoretical calculations [2] are broadly consistent in the $> 600 \text{ cm}^{-1}$ region with Gryaznova et al.

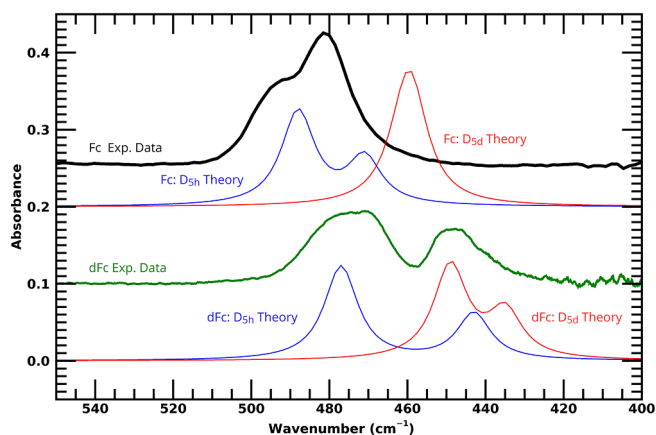


Fig. 2. Gas-phase relative absorbance of IR spectra of Fc (black, top, offset) and dFc (green, bottom), at 353 K, compared with DFT calculated IR spectra at 0 K [2] for D_{5h} (blue) and D_{5d} (red) in the gas-phase for Fc and $Fc - d^{10}$. Uncertainties (standard deviations) $\sigma_{sd} = 0.0006, 0.0011$ for the Fc and dFc spectra, respectively. The IR spectra of dFc is closer to the D_{5h} form, but the IR spectra look inconsistent with theory: the more intense band of Fc lies at lower wavenumber and the amplitudes appear different. (For interpretation of the references to colour in this figure legend, the reader is referred to the web version of this article.)

[34]. However, significantly, the bands in the key region 450 cm^{-1} are inconsistent between computations where they are dominated by Fe-related vibrations.

3. Experimental data

The experimental gas-phase deuterated ferrocene spectra (Fig. 2) show two clearly separated peaks in the band which roughly line up with the D_{5h} conformation, but with quite different separation of components and quite different broadening. Whilst the frequency splitting of two broad bands in the $450\text{--}500\text{ cm}^{-1}$ region is clear for Fc, the more intense band lies at the low wavenumber, which is predicted for the D_{5d} rotamer but with very narrow separation of components. Neither D_{5h} nor D_{5d} gas-phase predictions conform to the experimental observations. Similarly, the D_{5h} nor D_{5d} predictions are unable to explain the spectral variation with temperature of the dilute data (Fig. 3). Given the resolution and accuracy of our new data, interesting anomalies in the profiles include:

1. the gas phase profile appears to be inverted for the Fc singlet and doublet [18] (Fig. 3) – the intensities of the peaks are reversed;
2. the temperature series data (Fig. 3) show a complex profile structure and variation with temperature. These new experimental data sets are in more complex disagreement with a simple prediction

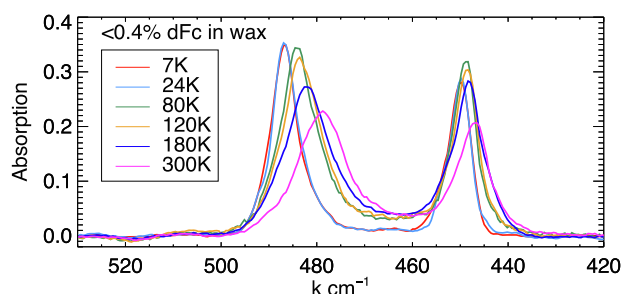
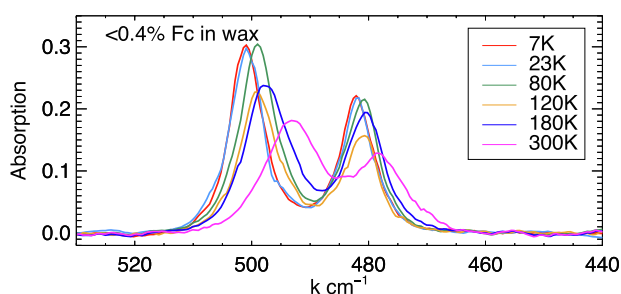


Fig. 3. Experimental IR spectra of Fc and dFc in solid (frozen) solutions over temperatures from room temperature down to 7 K, background-corrected. The complex temperature dependence of peak energy, centroid, band location, amplitude and area, and asymmetric broadening require advanced physical models and advanced theory. Standard deviation uncertainties are functions of the data repetition and variance. Typical values for dilute dFc in frozen paraffin wax solution for $T = 7\text{ K}, 24\text{ K}, 80\text{ K}, 120\text{ K}, 180\text{ K}, 300\text{ K}$ are $\sigma_{sd} = 0.0015, 0.0025, 0.0026, 0.0031, 0.0025, 0.0022$.

of theory, quite separately and inconsistently for the gas-phase data, the dilute system in wax, high temperatures and low temperatures for both Fc and dFc.

3. relative intensities appear quite different from theoretical expectations, whether for Fc or dFc, eclipsed or staggered, vapour or solution (Fig. 3 – i.e. the oscillator strengths of the peaks are anomalous, even for $T = 7\text{ K}$;

4. theoretically predicted profiles for the D_{5h} and D_{5d} conformations are offset in frequency compared with experimental profiles. These shifts might correspond to convergence and accuracy limits of DFT predictions. These complex variations show a pattern which can reveal the theory, quantum chemistry, structure and dynamics.

4. The ability to resolve hypotheses

This high quality data demonstrates the power of advanced infrared spectroscopy to probe the structure of disordered systems. Using goodness-of-fit (χ_r^2 analysis) with established uncertainty estimates and advanced hypotheses, we can investigate and explicitly discriminate between hypotheses:

- A Single Conformer Model (Hypothesis A) assumes that the sample can be well-modelled *either* as a purely eclipsed *or* as a purely staggered conformer. This has been the conclusion from many sources in the literature [6,7,17–19,24,20,38,25,26,22,27,40,29,30,33].
- A Mixed Conformer Model (Hypothesis B) assumes that the sample can be well-modelled by a mean dihedral angle between D_{5h} (0°) and D_{5d} (36°) [22,27,41,21]. *Or preferably*, as a mixture of ‘fully-eclipsed’ and ‘fully-staggered’ species [42,21]. This latter option might be used and extended to consider a Boltzmann factor between the two rotamers [1,43]. An extreme limit of this option would suggest free rotation of the Cp rings with no barrier, yielding an effective 50:50 mixture. Such a free rotation has been claimed in experiment and molecular dynamics simulations [44,24,40,29] at 300 K, but also that free rotation begins at liquid helium temperatures [45]. This hypothesis allows for frequency offsets for the eclipsed and staggered DFT predictions. These two hypotheses (A and B) cover almost all hypotheses and conclusions from past literature.
- An RCM Model (Hypothesis C) assumes the validity of the latest DFT predictions and introduces the concept of a potential energy surface between rotamers, with N vibrational levels between 0° and 36° . Populations of each vibrational level are given by assuming a Boltzmann distribution for the sample at temperature T , beginning an investigation into the Reaction Coordinate Method (RCM).
- The Advanced RCM Model (Hypothesis D) allows the key parametrisation to vary from predictions. This model allows optimisation of the IR relative peak amplitudes (oscillator strengths) at the

lowest temperature investigated, $T = 7$ K, first, closest to matching the theoretical calculations.

5. Eclipsed or staggered? A Single Conformer Model

The simplest model of Fc would be: (i) that the Fc or dFc system is either purely eclipsed (*Ec*) D_{5h} or purely staggered (*St*) D_{5d} ; and (ii) that the theoretical models exactly represent this ideal. In other words, the first model (Hypothesis A) represents the spectrum of Absorbance A versus ν (wavenumber in cm^{-1}), as Eqs. (1) or (2) (see Supp. material). The locations and offsets of the IR spectra are approximately aligned with the experimental data across the IR spectral range ($400\text{--}1200\text{ cm}^{-1}$) with modest 25 cm^{-1} offsets (Fig. 1). Theory has not been scaled nor offset to this point.

It is clear that neither the D_{5h} nor D_{5d} conformation theoretical band structure is able to represent the Fc spectra (Figs. 2 and 3), even including an energy offset. To model the band profiles of the conformations for both $Fc - d^{10}$ and $Fc - d^9$ compounds in terms of their isotopic composition, the fitting model needs to include additional Voigts to model the 10% contribution from $Fc - d^9$ in the sample (Table S6). The D_{5d} conformers ($Fc - d^{10}$ or $Fc - d^9$) possess a single broadened peak within experimental resolution. A pure D_{5h} conformation predicts the dominance of the first peak modestly, but the spectra are unable to match in terms of frequency offset, relative intensity and broadening. The spectra change dramatically with temperature and cannot match any model with a fixed ideal conformer (Fig. 3). Hence any Single Conformer Model is disproven for both Fc and dFc in the gas phase or frozen solution.

6. Mixed conformer model? Hypothesis B

Fitting a mixture of the D_{5h} and D_{5d} theoretical gas phase DFT computations at a given temperature would reveal the relative contributions of the conformations in this experimental observation. This allows an investigation beyond the facile Single Conformer Model and permits the investigation of the dependence of changes of conformation. This might give information on the energy difference between two stable minima on a potential surface. Hence the simplest Hypothesis B is (i) that the system is a mixture of purely D_{5h} and purely D_{5d} Fc or dFc; and (ii) that the theoretical models exactly represent this ideal, with likely frequency offsets required for comparison with DFT gas-phase theory (see Supp. material).

This series of possible models suggest that Fc is a two-component mixture; or similarly that the angle between the two parallel Cp rings is neither 0° nor 36° but some angle in between. Crystallographic studies primarily observe lattice positions in a regular crystal, and by extension predict regular space-group symmetry, bond lengths and bond angles, naturally affected by crystal packing. In the presence of significant disorder, these can be interpreted as average site occupations and bond lengths in a static rather than dynamic sense. The idea of a two-component mixture might naturally lend itself to an interpretation of a mean dihedral rotation angle between the Cp rings, so that if a mixture reported 80% D_{5h} and 20% D_{5d} , this might correspond to an average rotation angle of $36^\circ \times 20\% = 7.2^\circ$. Crystal disorder might affect this interpretation; or the minimum potential could correspond to a 7.2° rotation angle. This directly implicates dominance of a particular conformer. Results claim to span the full range from $0^\circ(D_{5h})$ to $36^\circ(D_{5d})$ (Table S3).

6.1. Mixed conformer model for gas phase

The theoretical convergence for one conformation (D_{5h}) may be different from that for the other conformation (D_{5d}). Having independent frequency offsets $\delta\nu_{Ec}$ and $\delta\nu_{St}$ for the eclipsed and staggered conformers respectively between the gas-phase DFT and the experimental spectra is necessary to fit the Fc gas phase spectra well. This is

reflected by a significant improvement in the standard goodness-of-fit parameter from statistical analysis, $\chi_r^2 \sim 17.9$ (Fig. S12).

In the case of dFc (Fig. 2), fitting a frequency offset for each component improves the fit somewhat, but remains a very poor fit ($\chi_r^2 \sim 194$) and does not change the fraction of the D_{5d} conformation, which remains minor. The inconsistency between the 50% mix for the gas phase Fc data and the 95% value for dFc, and the inequivalence of the relative frequency offsets, argues for the inadequacy of the model. In other words, Fc and dFc should fit with similar percentages of each conformer at gas phase temperatures.

6.2. Mixed conformer model for temperature series

For a single frequency offset between theory and experiment for the dilute Fc spectra in wax, the fitted profiles do not agree with experimental data. When each conformer is given an independent offset, the D_{5h} conformer appears dominant and predicts the correct relative intensity of the peaks across the measured temperature range (Fig. S13). The fits are in quite good agreement with χ_r^2 of 9.0–11.9 for each temperature. The small D_{5d} fraction appears to have a uniform offset from theory but quite high at $20.5(2)\text{--}21.6(4)\text{ cm}^{-1}$; while the dominant D_{5h} conformer has a fitted offset from theory which varies with temperature from $11.8(3)\text{ cm}^{-1}$ for $T = 7$ K to $4.6(4)\text{ cm}^{-1}$ for $T = 300$ K. The percentage D_{5d} varies from 20% at lowest temperature to about 35% at $T = 300$ K. Variation of these parameters with temperature is an exploration of the limitations of the model and of the required components of an improved model. In other words, physical parameters such as the offset between experiment and theory should be a constant rather than a function of temperature.

The same Mixed Conformer Model is applied to the D_{5h} and D_{5d} conformations in the IR spectra of $Fc - d^{10}$ using Eq. (4) (Supp. material). For the dFc temperature series of data, the theoretical D_{5d} profile cannot fit the data at all (Fig. S14), with imputed contributions of 0% at low temperature and up to 14% for $T = 300$ K. $\chi_r^2 = 147$ for $T = 7$ K data set, not much improved for $T = 300$ K with $\chi_r^2 = 56$. The relative intensities do not agree and do not match for any temperature.

We observe significant discrepancy at $T = 7$ K where the conformation might be unique and is predicted and observed to be mainly D_{5h} . Therefore, the theoretically calculated relative intensities (Table S6) for the gas-phase spectra were further investigated by fitting the lowest temperature (7 K) IR spectra using band frequencies only for the D_{5h} conformations (i.e. $I_{St,7K} = 0$). A correction factor of 1.37 ± 0.02 was fitted for the singlet intensity of the D_{5h} dFc, and propagated the correction to fit the spectra at all temperatures. It was necessary to fit a correction scaling factor of 1.81 ± 0.02 to the intensity for the singlet for Fc. This intensity correction factor was used to fit the spectra at all temperatures. The correction of the intensity is insufficient to obtain satisfactory agreement at 120 K and 300 K (χ_r^2 of 53 and 123 for Fc and dFc for example) and further improvement of the modelling is required. The evidence presented herein demonstrates that these models (Single Conformer Models and Mixed Conformer Models, Hypotheses A and B) are invalid despite covering almost all conclusions from past literature.

7. RCM model: Hypothesis C

If we consider the potential surface of the rotation around the Cp ring between conformations, we should expect a periodic potential with either two stable conformations or a stable conformation and a transition state conformation (Fig. 4). A key parameter from literature – the barrier height ΔE to the internal rotation of the Cp rings – has been investigated using different techniques and media.

The electron scattering technique was applied to gaseous Fc at high temperatures 673 K [46], and 413 K [24] to investigate the energy barrier to internal rotation of the Cp rings. The scattering pattern from the gas at 673 K found no rotational barrier [46]; however, Fc

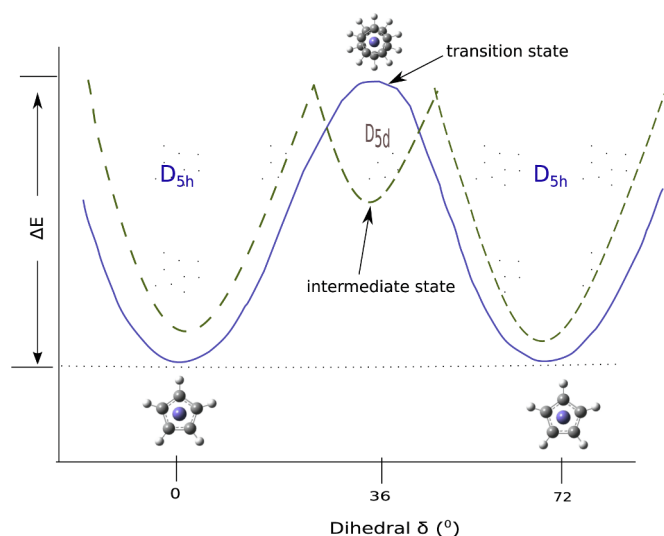


Fig. 4. Schematic of the possible relative energy change as one Cp ring rotating by a dihedral angle ϕ with respect to the absorber axis (connecting the centres of two Cp rings) in the periodic formation process of two conformations (eclipsed and staggered) of ferrocene. Due to the pentagon structure of the Cp rings, every 36° rotation of the dihedral angle rotates from one conformation to the other.

decomposes around this temperature. An electron scattering study of gaseous Fc at 413 K [24] found a barrier of $3.8 \pm 1.3 \text{ kJ mol}^{-1}$ to the internal rotation. Although the refinement of the experimental intensity curves weakly supported the D_{5h} conformation, the imputed barrier was low and with large uncertainty (34%). It has been suggested that the value of ΔE is much larger for the orthorhombic phase though with a large 48% uncertainty ($33 \pm 16 \text{ kJ mol}^{-1}$) [23] and with strong disagreement with measurements using NMR [47]. The barrier is reported to be relatively small in triclinic ($T < 164 \text{ K}$) and smaller still in monoclinic phases ($T > 164 \text{ K}$), but this casts doubt on the orthorhombic result and structure. If the orthorhombic estimate of 10.1 kJ mol^{-1} from XRD is accurate, then there is perhaps no change of barrier height in the phase transition from orthorhombic to triclinic. Conversely, if the ADP estimate for triclinic and monoclinic is accurate, then there may be no change of barrier height in the phase transition from triclinic to monoclinic.

For different DFT functionals, the energy of the rotational barrier varies significantly [29]. The dynamics are temperature dependent, so understanding the rotation dynamics requires measurements across a

series of temperatures. If either model in Fig. 4 for Fc and dFc is valid, then the potential appears like a simple harmonic oscillator for most rotation angles. The evidence of the spectra so far presented implies that at low temperature the D_{5h} conformer is predominant.

The profiles along the potential surfaces between the conformers can be obtained using the difference $\Delta\nu_j = \nu_{j,St} - \nu_{j,Ec}$ between the D_{5h} and D_{5d} calculated band frequencies ν , the number of vibrational levels N and the rotation angle ϕ from $0^\circ - 36^\circ$ for the interconversion between the rotamers. The intensities for the corresponding component profiles can be derived by implementing the probability of a Boltzmann distribution with a transition state (see Supp. material).

The lowest wavenumber vibrational mode for the D_{5h} form of Fc is calculated to be $\nu_1 = 17.26 \text{ cm}^{-1}$, whilst the D_{5d} form in the transition state higher by a predicted 2.53 kJ mol^{-1} provided an imaginary frequency of $\nu_1 = -29.9 \text{ cm}^{-1}$. This provides a prescription for a hypothesised potential energy surface for the interconversion between the rotamers [1]. Table 1 summarises required parameters from DFT to fit the observed IR spectra of Fc and dFc.

For the dilute Fc and the dilute dFc temperature series, this RCM Model (Hypothesis C) using theoretical DFT parameters is well-formed but leads to a poor fit with $\chi_r^2 \sim 200$, because of limitations of the DFT prediction and computation of the frequencies. The data require offsets for the eclipsed conformation for the singlet and doublet frequencies and for the hypothesised transition state staggered conformation, as revealed by the low-temperature experimental data. An overall scale is necessary to relate the theoretical intensities from km mol^{-1} to absorbance, assuming that the spectrum lies in the linear regime and avoids saturation. Whilst the model is persuasive, this compelling evidence requires a novel model to explain the dynamics of ferrocene.

8. Advanced RCM Model in solution: Hypothesis D

This model hypothesis allows parameters to vary from the DFT predictions, especially because of the theoretical uncertainty and convergence limitations. For the very lowest temperatures (7 K), only the lowest occupied mode, the ground state D_{5h} mode, will contribute. Hence several critical parameters are found or fitted best in the lowest temperature data, yet should be consistent and stable for all temperatures, viz. $\nu_7; \nu_8; \nu_9 (D_{5h}), I_7; I_8; I_9 (D_{5h})$. Conversely, parameters $\nu_7; \nu_8; \nu_9 (D_{5d}), I_7; I_8; I_9 (D_{5d}), \nu_1$, and the barrier height ΔE or $\Delta\nu = \nu_1 N$, cannot be determined from the lowest temperature data set because only the lowest ground state mode is occupied at 7 K. For deuterated ferrocene, both d^{10} and d^9 forms must be included in approximately the ratio given by the experimental sample preparation specification 9:1. As with the two-component model, especially for the lowest temperature

Table 1
DFT predictions and literature values of chemically significant parameters.‡

Band frequencies	D_{5h}				D_{5d}			
	ν_1	ν_7	ν_8	ν_9	ν_1	ν_7	ν_8	ν_9
Fc, gas-phase DFT, ν (cm^{-1})	17.27	471.2278	488.7036	488.7156	-29.88	461.2664	459.5262	459.5285
Intensities, I (km/mol)		17.7516	22.2985	22.2904		17.3881	25.5412	25.5403
ΔE_{DFT}		211.1 cm^{-1} , 2.527 kJ mol^{-1}						
# of bound vibrational levels		$N = 12$						
Fc - d^{10} , gas-phase DFT, ν (cm^{-1})	15.57	443.1440	477.1403	477.1522	-26.95	435.7617	449.8169	449.8191
Intensities, I (km/mol)		23.6745	23.2981	23.2906		22.7629	26.2227	26.2219
ΔE_{DFT}		216.4 cm^{-1} , 2.590 kJ mol^{-1}						
# of bound vibrational levels		$N = 14$						
Fc - d^9 , gas-phase DFT, ν (cm^{-1})	15.72	445.5237	477.9126	478.4622	-27.21	437.9741	450.4575	451.0659
Intensities, I (km/mol)		23.1164	23.1919	23.1248		22.2765	26.128	26.1
ΔE_{DFT}		215.7 cm^{-1} , 2.582 kJ mol^{-1}						
# of bound vibrational levels		$N = 14$						

‡ ν_1 , barrier height from DFT, $\Delta E_{DFT} = E_{St} - E_{Ec}$, $N = \text{Int}\left(\frac{\Delta E}{h\nu_1}\right)$, this work [2,48]; Ref. [1] estimated $\nu_1 \sim 25 \text{ cm}^{-1}$ and $\Delta E \sim 6 \text{ kJ mol}^{-1}$.

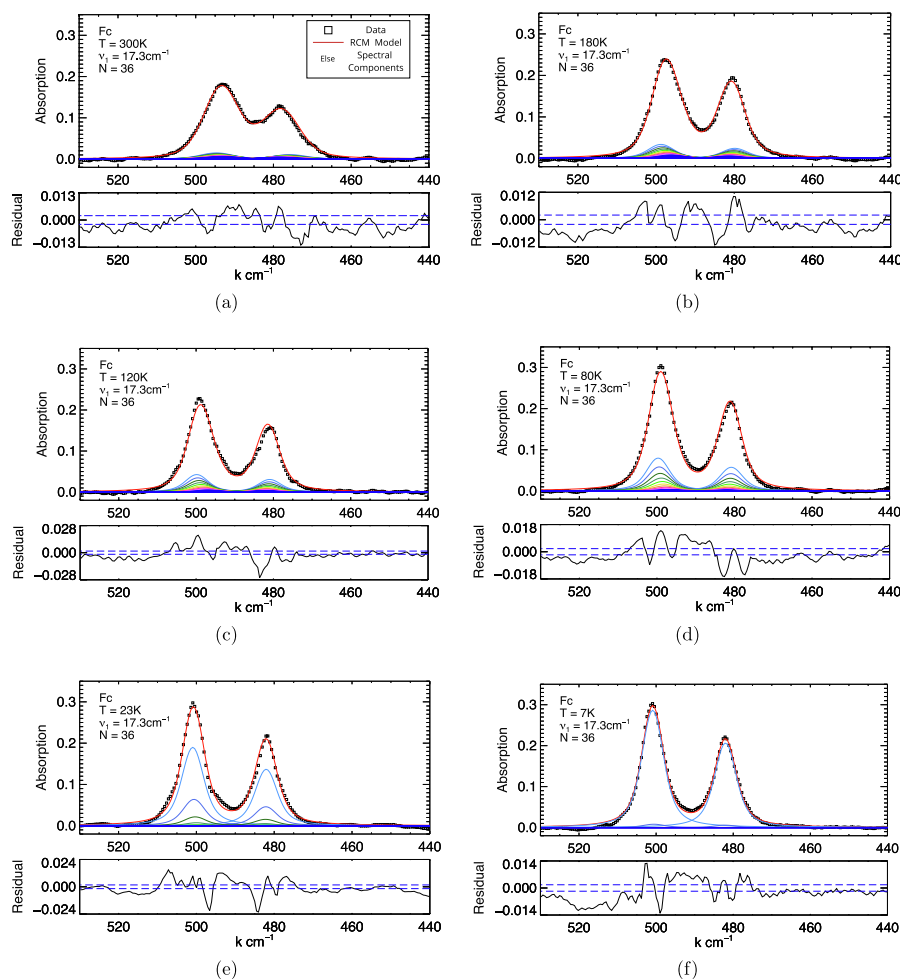


Fig. 5. IR spectra of dilute Fc in wax measured, and using the Advanced RCM Model (Hypothesis D). Outstanding quantitative agreement is found with RCM and advanced DFT, with an excellent fit at low temperatures with a χ_r^2 of 9.4 at 7 K, 12.2 at 23 K, 7.3 at 80 K, 10.6 at 120 K, 4.7 at 180 K, and even 3.5 at 300 K. Data = squares. RCM result = red line. Spectral components in colours. Residual in lower figure with ± 1 standard error dashed line. (For interpretation of the references to colour in this figure legend, the reader is referred to the web version of this article.)

data set for dFc, but also for Fc, this requires a parameter $I_{8,9}/I_7$. Neither $I_{8,9}/I_7$ nor an offset $\nu_{8,9} - \nu_7$ were investigated earlier [1]; investigation of these permits quantitative agreement of theory and experiment. The data requires a parameter to measure the ratio of $I_{d^9}/I_{d^{10}}$. Freeing each of these assumptions led to continuously improved fits and structural agreement.

Apart from the broadening, the advanced reaction coordinate approach has all parameters consistent for all temperatures (Figs. 5, 6, Table 2) although there is a small variation of frequency with increasing temperature: Fc: $\delta\nu_{EC}$: $12.20(2) \text{ cm}^{-1}$ decreases by circa 6.2 cm^{-1} with increasing temperature across the series and dFc: $\delta\nu_{EC}$: $8.64(5) \text{ cm}^{-1}$ decreases by circa $3.47(8) \text{ cm}^{-1}$ with increasing temperature across the series. This variation is observed experimentally in nearly spectral lines and is likely indicative of thermal expansion. Compared with any alternate approach or hypothesis, the improved and quantitative agreement is remarkable. The tabulated parameters are sparse and tightly linked to the predicted advanced theory from DFT.

The stereochemistry associated with the Cp rings for Fc and dFc is expected to be the same, and the ordering of the energies of the vibrational modes of Fc should be compatible with that for dFc, following the expected reduced mass dependencies. A satisfactory interpretation of the spectra can be made by constraining ν_1 in the fitted models for Fc and dFc corresponding to the amplitude of harmonic motion for a given normal mode. Theory calculates $\nu_1 = 17.27 \text{ cm}^{-1}$ for Fc, $\nu_1 = 15.57 \text{ cm}^{-1}$ for Fc - d^{10} and $\nu_1 = 15.72 \text{ cm}^{-1}$ for Fc - d^9 , with the calculated

reduced mass dependency already incorporated. Chhor et al. [40] suggest that theoretical isotopic ratios of the lowest vibrational frequency between Fc and dFc might be 1.11. Lippincott et al. [18] noted different values for asymmetric ring metal stretch 1.04 (the singlet) or asymmetric ring tilt (1.01–1.09). The model is able to successfully maintain the DFT values and ratios, though the data do not clearly discriminate between different values. In fact, results are mainly sensitive to the barrier height or equivalently to the number of vibrational levels N below the barrier height. The data suggests ΔE and hence N significantly larger than some DFT theory [29,30,48,39] and some results interpreted from experiment [24,23,49,28] but well within the range interpreted from different experimental techniques [50,42,27,51,47,23,28]. The estimated barrier height for the molecules for Fc is 7.4 kJ.mol^{-1} , and for Fc - d^{10} is 6.3 kJ.mol^{-1} , and for Fc - d^9 is 6.4 kJ.mol^{-1} . Hence N was optimised to be 36 for Fc and 34 for Fc - d^{10} . N and the barrier height are not tightly tied down by theory or experiment.

9. Advanced RCM IR gas-phase spectra: Hypothesis D

Whilst this agreement in solution is compelling for the Advanced RCM Model, the gas-phase spectra represent an even more difficult challenge. This is a different quantum chemistry system, where the molecule is not relatively isolated in a frozen solvent but is isolated in a gas-phase system at high temperatures $T = 388 \text{ K}$. Statistics, adsorption and background subtraction can be more challenging. The model for

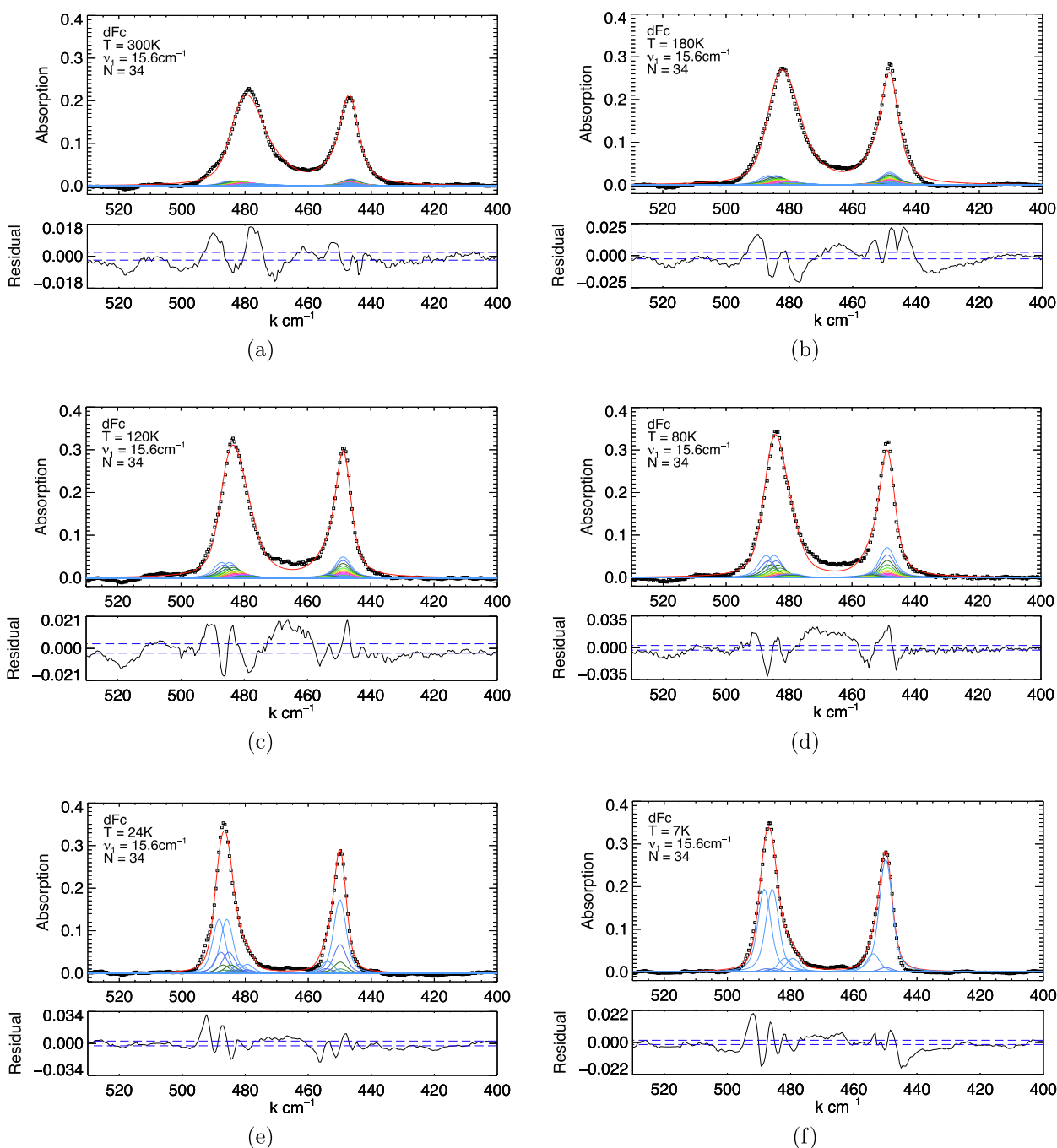


Fig. 6. IR spectra of dilute dFc in wax measured, and using the Advanced RCM Model (Hypothesis D). Outstanding quantitative agreement is found with RCM and advanced DFT, with an excellent fit at low temperatures with a χ_r^2 of 14.6 at 7 K, 6.8 at 24 K, 13.6 at 80 K, 6.1 at 120 K, 10.5 at 180 K, and even 6.7 at 300 K.

solution may not agree for high temperature gas phase for a range of reasons – anharmonicity, multiple modes; and phase. Whilst the key DFT computations were for an isolated gas, they were also intended for $T = 0 \text{ K}$; so some details of the model might be required to change.

The spectra are fitted quantitatively, extremely well, with the *same* vibrational level spacing $\Delta\nu = \nu_1 = 17.27 \text{ cm}^{-1}$ as for the Fc temperature series in solvent, the *same* barrier height and the *same* number of possible vibrational levels below the barrier, $N = 36$ for Fc (Fig. 7). The theoretical offset for the frequency for the eclipsed conformer $\delta\nu_{Ec, Fc} = 9.60(2) \text{ cm}^{-1}$ also lies inside the range observed for the temperature series for the wax solvent. As expected, the line broadening is greater for the gas phase, with the Lorentzian broadening width w_L ill-defined at 9.0 cm^{-1} and the Gaussian width w_G well-defined as

$2.4(6) \text{ cm}^{-1}$. The singlet-to-doublet scaling is a bit higher than for the solvent, $I_{8,9}/I_7 = 2.39(8)$ and the offset between the doublet frequency and the singlet frequency is again small $\delta\nu_{Ec,8,9-7} = -2.8(2) \text{ cm}^{-1}$.

Even more impressive is the spectral modelling of the gas-phase dFc. The earlier RCM Model (Hypothesis C; Fig. S15) using advanced DFT theoretical predictions including frequency corrections for offset and scale yielded a much better agreement with experiment than the Mixed Conformer Model (Hypothesis B). However, Advanced RCM improves upon this dramatically to yield $\chi_r^2 \approx 24$ (Fig. 8), disproving these earlier and popular hypotheses. ν_1 and N and barrier height are able to be consistent with the low temperature series results for dFc. (Ref. [1] estimated $\Delta E \sim 1\text{--}3 \text{ kJ mol}^{-1}$ for gas spectra versus $\Delta E \sim 6 \text{ kJ mol}^{-1}$ for lower temperature solution spectra).

Table 2
Modelled experimental frequencies, relative intensities, uncertainties of chemically significant parameters.‡

Band frequencies	D_{5h}				D_{5d}		
	ν_1	ν_7	ν_8	ν_9	ν_7	ν_8	ν_9
Fc , gas-phase fitted data, ν (cm^{-1})	17.27 f	482.04(4)	500.90(2)	500.92(2)	485.04(30)	489.83(20)	489.83(20)
Intensities, I (km/mol)		32.13(30) \dagger	22.2985	22.2904			
$\Delta E_{\text{Experiment}}$		7.44 kJ mol $^{-1}$		$N = 36$			
$Fc - d^{10}$, gas-phase fitted data, ν (cm^{-1})	15.57 f	449.87(9)	485.78(5)	488.30(9)	448.41(40)	463.92(30)	466.43(30)
Intensities, I (km/mol)		31.72(20) \dagger	23.2981	23.2906			
$\Delta E_{\text{Experiment}}$		6.34 kJ mol $^{-1}$		$N = 34$			
$Fc - d^9$, gas-phase fitted data, ν (cm^{-1})	15.72 f	453.87(20)	479.29(20)	482.35(20)	468.09(200)	477.30(100)	480.42(100)
Intensities, I (km/mol)		46.2(30)	34.6(20)	34.6(20)			
$\Delta E_{\text{Experiment}}$		6.40 kJ mol $^{-1}$		$N = 34$			

‡: Barrier height $\Delta E = E_{S_1} - E_{E_C}$, $N = \text{Int}(\frac{\Delta E}{h\nu_1})$. f : fixed, \dagger : relative intensity ratio, N : number of bound vibrational levels.

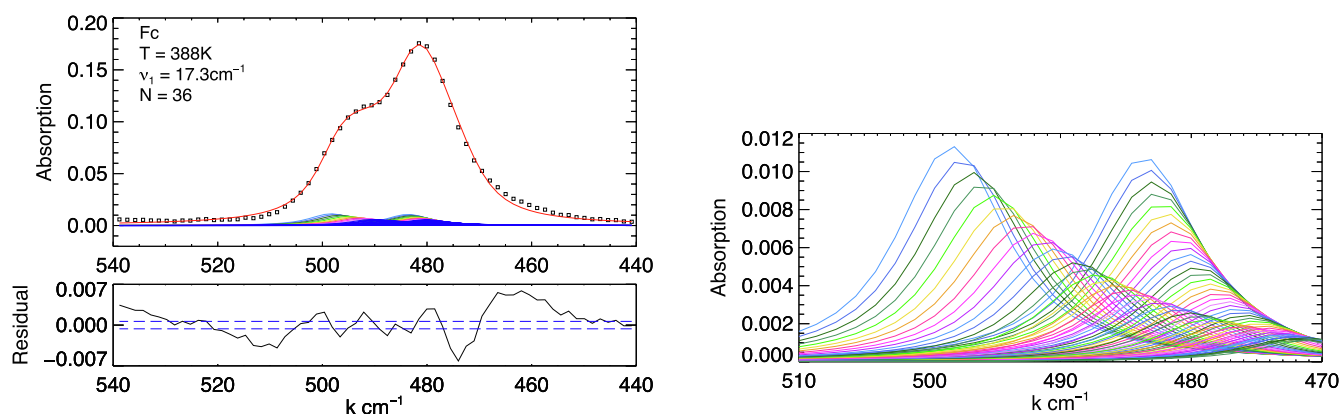


Fig. 7. Left: The Advanced RCM Model is extremely successful for the high-temperature gas-phase data for ferrocene for $T = 388$ K with $t = 18.8$. Right: Inset of model components.

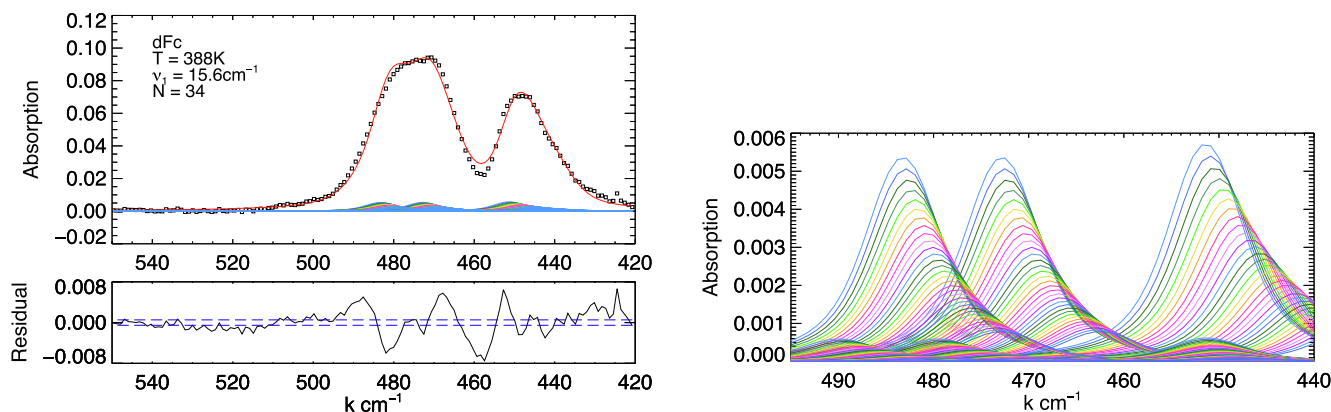


Fig. 8. Left: dFc gas phase modelling for $T = 388$ K using the Advanced RCM Model, Hypothesis D, allowing experiment to drive the understanding of DFT theoretical predictions. The improvement in agreement, with $\chi_r^2 \approx 24$, is a major success of RCM. Right: Inset of model components.

Offsets of frequencies for D_{5d} and D_{5h} conformers are similar, broadening as expected is a little larger, and scaling is broadly consistent. There is a significant change in the singlet-doublet frequency offset, the separation of the doublet, and the $Fc - d^9$ offset, each about 10 cm^{-1} ; as might be expected due to the different quantum system and environment.

10. Results and discussion

The first question of our inquiry was whether we could tell between the eclipsed and staggered conformers. We conclude that the lowest-

temperature IR spectra of dilute Fc is dominated by the D_{5h} eclipsed conformation. As the temperature increases, we predict and observe an increasing population of occupied modes along the reaction coordinate towards the D_{5d} frequencies. In order to fit the Fc and dFc spectra across the temperature series we must allow:

- (i) An energy offset ($10\text{--}30 \text{ cm}^{-1}$) from DFT theory for each of the D_{5h} and D_{5d} conformers. This is required and expected (Fig. 1) as an indication and level of convergence of theory. The D_{5h} offset(s) indicate the main peak location at low temperature; and the D_{5d} offset (s) indicate the developing asymmetry of the profile as the

temperature increases and more modes are occupied.

(ii) The D_{5h} singlet intensity compared with the doublet intensity is much higher than predicted (a factor of ~ 1.81 for Fc and 1.34 for dFc), optimised (fitted) to the lowest temperature data (7 K). This is similar for both experimental data sets at $T = 7$ K and is an indication of the convergence of the oscillator strengths from theory. This ratio is consistent (a common parameter) for all temperature data.

(iii) Refinement (fitting) of the percentage of the $Fc - d^9$ to $Fc - d^{10}$ in the dFc sample from the specification of 1:9. The factor correction of 1.49 suggests that the sample was not quite so well deuterated as claimed but within the uncertainty of the isotopic purification.

(iv) A small offset (1.4 cm^{-1} for Fc or 1.8 cm^{-1} for dFc) between the singlet and doublet, optimised (fitted) to the lowest temperature data available (7 K). This is well within the convergence uncertainty, across the $20\text{--}30 \text{ cm}^{-1}$ spectral range of the profile. Similarly, small relative frequency offsets are required for the D_{5d} conformer DFT predictions fitted from the higher temperature series.

(v) For dFc, separate offsets and scaling factors are required for $Fc - d^9$ and $Fc - d^{10}$. This model predicts or allows frequencies following exactly the isotopic ratios predicted by DFT. Whilst the $Fc - d^9$ component is relatively minor, and the corresponding offsets appear quite small, the offsets are essential for convergence of experiment with theory.

(vi) Modest Gaussian and Lorentzian widths $w_G \sim 3 - 5.7 \text{ cm}^{-1}$ and $w_L \sim 2 - 5.3 \text{ cm}^{-1}$ for component Voigt profiles, with broadening increasing with temperature as expected.

(vii) The mode separation ν_1 currently appears well defended by DFT theory, although the barrier height between D_{5h} and D_{5d} $\Delta E \sim N\nu_1$ appears to be more than double that theoretically predicted by some advanced DFT and less than a variety of other measurements. The uncertainty of ν_1 and N is significant given these data sets. The more robust parameter experimentally is ΔE . The remarkable new consistency of the predicted and experimental spectra for Fc and dFc, for temperature series in solution and for the high-temperature gas-phase measurements, argues strongly for the success of the Advanced RCM model and analysis. A careful reader will note that χ_r^2 is not unity; so indeed the estimated uncertainties suggest more physical understanding of the quantum chemistry might continue to be rewarding; yet it is orders of magnitude improved over past work and it is robust and well-defined.

Early research of IR spectra claimed that Fc was dominated by the D_{5d} conformation, but the present analysis of gas-phase, and temperature dependent IR spectra of Fc and dFc conclude that the spectra is contributed by vibrational excitations along the reaction coordinate and not by any mixture of conformers, using high quality DFT calculations. The IR spectra of Fc from the gas-phase measurements have different profiles from calculated or observed spectra in solutions of differing polarity, but the frequency splitting is clear (blue line; Fig. 2), and in agreement with eclipsed ferrocene.

The analysis of the temperature-dependent IR spectra indicates that low temperature (<80 K) IR spectra of Fc and dFc are dominated by the D_{5h} conformer in the ground vibrational state, while vibrational occupation along the reaction coordinate to D_{5d} effectively contributes increasingly via higher modes above 80 K. The spectral shifts $\Delta\nu$ of the key profiles determined from the fits are in agreement with the theoretically calculated spectral shift for the eclipsed conformations. Whilst anharmonicity is expected at some level at higher temperatures, this is minor or negligible across the full range of temperatures investigated herein, possibly because of the symmetry and stability of the Cp rings. Some small discrepancies can be seen in individual profiles. At higher temperatures we might expect possible off-axis excitation modes beginning with $\nu_{2,3} \approx 167 \text{ cm}^{-1}$ a near-doublet. Most molecules will exhibit anharmonicity from the oscillator potential well, or indeed from

the cyclic and near-sinusoidal nature of the ring potential. The model does not observe a second minimum in the reaction coordinate and theory does not predict it either, yet experimentally this is not yet ruled out. At high energies continuum occupied levels may permit free rotation. We do not observe evidence for these in the current spectra and modelling, but we do not rule out the possibility that these might play a role in the understanding of these complex systems.

The Advanced Reaction Coordinate Method (RCM) for the transition (vibrational level) model has significant advantages over any Mixed Conformer Model, including a natural constraint to follow a Boltzmann population for excited energy levels. We have determined plausible error bars and we test hypotheses using least-squares minimisation and χ_r^2 as a goodness-of-fit. This is a new methodology for analysis of these spectra [3]. The quality of the data down to 7 K, the nature of the pre-processing, the use of wax as a solid solution solvent, and the approach to understanding the temperature series are novel. Individual DFT predictions cannot explain the experimental spectra, even at the lowest temperature in a qualitative sense; at higher temperatures it becomes clear that the observed conformer and structure is dynamic. The development of RCM can achieve remarkable consistency in the explanation across a full range of temperature.

11. Conclusions

Our high quality FTIR experimental data with uncertainty across a wide temperature series allows quantitative investigation of the quantum chemistry, reaction surface and dynamics of Fc and dFc. The Reaction Coordinate Method and the developed model, presented herein, predicts the detailed spectrum and spectral changes across a wide range of energy including the highest temperatures, and even for a different phase, consistently. Compared with qualitative fits or direct DFT fits the model is extremely persuasive.

Conclusions from the literature that Fc is purely eclipsed D_{5h} or purely staggered D_{5d} (Hypothesis A) are proven invalid from the data. Conclusions (at least for non-crystalline Fc) of a mean angle between Cp rings; or a mixture of D_{5h} and D_{5d} , even with a temperature-dependence and possibly from a direct application of a Boltzmann factor, (Hypothesis B) is disproven by the data. Hence we are forced to a model of vibrational levels, the Reaction Coordinate Method, in a (repeating) simple harmonic oscillator potential well.

We explain the inversion of the ordering of the gas phase Fc spectra compared to DFT eclipsed theory; the large discrepancy of doublet and singlet intensities measured compared with DFT predictions by factors of 1.34(1) and 1.81(2) for Fc and dFc; and measure and determine the specific frequency offsets from DFT required to explain the spectra. We observe and explain non-uniform broadening of singlet and doublet profiles with increasing temperature, and are able to represent the reduced mass ratios of the lowest vibrational modes for Fc and dFc of 1.11 for ν_1 for Fc to $Fc - d^9$ and of 1.10 for Fc to $Fc - d^{10}$. For dFc, we measure the purity of deuteration of the sample to be 98.5% with a model-based uncertainty of about 0.1%, rather than the supplier value 98.9% based on NMR, illustrating the sensitivity of an independent quantified diagnostic for the purity of deuteration. There is remarkable agreement for a model of D_{5h} minimum, vibrationally occupied levels, and a transition D_{5d} state with the data. We estimate ΔE is perhaps 7.4 and 6.3 $\text{kJ}\cdot\text{mol}^{-1}$ for Fc and $Fc - d^{10}$ respectively, double the estimates from some theory [2]. There is also a question of DFT convergence of such energy differences. Hence the result obtained is consistent with the variation reported. For dFc, we measure the purity of deuteration of the sample to be 98.5% rather than the supplier value 98.9%, illustrating the sensitivity of an independent quantified diagnostic for the purity of deuteration. These new techniques are sensitive discriminants of alternate models and chemical systems, which argues for wider application to other complex or impenetrable problems across fields arising for numerous other solutions, frozen or at room temperature.

CRediT authorship contribution statement

R.M. Trevorah: Formal analysis, Writing - original draft, Writing - review & editing. **N.T.T. Tran:** Formal analysis, Writing - original draft, Writing - review & editing. **D.R.T. Appadoo:** Investigation, Methodology, Writing - review & editing. **F. Wang:** Investigation, Methodology, Writing - review & editing. **C.T. Chantler:** Supervision, Conceptualization, Formal analysis, Writing - original draft, Writing - review & editing.

Acknowledgement

This research was undertaken on the THz/Far-IR beamline at the Australian Synchrotron, Victoria, Australia. We acknowledge the Australian Research Council (ARC) and the science faculty of the University of Melbourne for funding this work. This research is supported by the AINSE Honours Scholarship Program. We acknowledge M. T. Islam, S. Islam and S. P. Best for their experimental and conceptual contributions to this work. In particular, this work and development would not have been possible without the experimental drive and insight of S. P. Best.

Appendix A. Supplementary data

Supplementary data associated with this article can be found, in the online version, at <https://doi.org/10.1016/j.ica.2020.119491>.

References

- [1] S.P. Best, F. Wang, M.T. Islam, S. Islam, D. Appadoo, R.M. Trevorah, C.T. Chantler, Reinterpretation of dynamic vibrational spectroscopy to determine the molecular structure and dynamics of ferrocene, *Chem. Eur. J.* 22 (2016) 18019–18026.
- [2] N. Mohammadi, A. Ganesan, C.T. Chantler, F. Wang, Differentiation of ferrocene D_{5d} and D_{5h} conformers using IR spectroscopy, *J. Organomet. Chem.* 713 (2012) 51–59.
- [3] M.T. Islam, R.M. Trevorah, D.R. Appadoo, S.P. Best, C.T. Chantler, Methods and methodology for FTIR spectral correction of channel spectra and uncertainty, applied to ferrocene, *Spectrochim. Acta Part A: Mol. Biomol. Spectroscopy* 177 (2017) 86–92.
- [4] T.J. Kealy, P.L. Pauson, A new type of organo-iron compound, *Nature* 168 (1951) 1039–1040.
- [5] A. Miller, J.A. Tebboth, F. Tremaine, 114 Dicyclopentadienyliron, *J. Chem. Soc.* (1952) 632–635.
- [6] J.A. Page, G. Wilkinson, The polarographic chemistry of ferrocene, ruthenocene and the metal hydrocarbon ions, *J. Am. Chem. Soc.* 74 (1952) 6149–6150.
- [7] E.O. Fischer, W. Pfab, Cyclopentadien-metallkomplexe ein neuer Typ metallorganischer Verbindungen, *Z. Naturforschung Sect. B J. Chem. Sci.* 7 (1952) 377–379.
- [8] J.D. Dunitz, L.E. Orgel, Bix-cyclopentadienyl iron: a molecular sandwich, *Nature* 171 (1953) 121–122.
- [9] P.F. Eiland, R. Pepinsky, X-ray examination of iron biscyclopentadienyl, *J. Am. Chem. Soc.* 74 (1952) 4971.
- [10] J.D. Dunitz, L.E. Orgel, A. Rich, The crystal structure of ferrocene, *Acta Crystallogr. A* 9 (1956) 373–375.
- [11] J.I. Seeman, S. Cantrill, Wrong but seminal, *Nature Chem.* 8 (2016) 193–200.
- [12] D. Conroy, A. Moissala, S. Cardoso, A. Windle, J. Davidson, Carbon nanotube reactor: ferrocene decomposition, iron particle growth, nanotube aggregation and scale-up, *Chem. Eng. Sci.* 65 (2010) 2965–2977.
- [13] T.S. Chao, E.H. Owston, Iron-containing motor fuel compositions and method for using same (1978), <https://www.google.com/patents/US4104036>.
- [14] N. Metzler-Nolte, M. Salmann, The bioorganometallic chemistry of ferrocene, *Ferrocenes: Ligands Mater. Biomol.* (2008) 499–639.
- [15] S. Top, B. Dauer, J. Vaissermann, G. Jaouen, Facile route to ferrocifen, 1-[4-(2-dimethylaminoethoxy)]-1-(phenyl)-2-ferrocenyl-but-1-ene, first organometallic analogue of tamoxifen, by the McMurry reaction, *J. Organomet. Chem.* 541 (1997) 355–361.
- [16] S. Top, A. Vessières, G. Leclercq, J. Quivy, J. Tang, J. Vaissermann, M. Huché, G. Jaouen, Synthesis, biochemical properties and molecular modelling studies of organometallic specific estrogen receptor modulators (SERMs), the ferrocifens and hydroxyferrocifens: evidence for an antiproliferative effect of hydroxyferrocifens on both hormone-depen, *Chem. Eur. J.* 9 (2003) 5223–5236.
- [17] E.R. Lippincott, R.D. Nelson, The vibrational spectra and structure of ferrocene and ruthenocene, *J. Chem. Phys.* 21 (1953) 1307–1308.
- [18] E.R. Lippincott, R.D. Nelson, The vibrational spectra and structure of ferrocene and ruthenocene, *Spectrochim. Acta* 10 (1958) 307–329.
- [19] W.K. Winter, B. Curnutte Jr, S.E. Whitcomb, The infrared spectrum and structure of crystalline ferrocene, *Spectrochim. Acta* 15 (1959) 1085–1102.
- [20] I.J. Hyams, A. Ron, Infrared study of the lambda transition and molecular configuration in crystalline ferrocene, *J. Chem. Phys.* 59 (1973) 3027.
- [21] C.P. Brock, Y. Fu, Rigid-body disorder models for the high-temperature phase of ferrocene, *Acta Crystallogr. Sect. B: Struct. Sci.* 53 (1997) 928–938.
- [22] P. Seiler, J.D. Dunitz, The structure of triclinic ferrocene at 101, 123 and 148 K, *Acta Crystallogr. Sect. B: Struct. Crystallogr. Cryst. Chem.* 35 (1979) 2020–2032.
- [23] E. Maverick, J.D. Dunitz, Rotation barriers in crystals from atomic displacement parameters, *Mol. Phys.* 62 (1987) 451–459.
- [24] A. Haaland, J. Nilsson, The determination of barriers to internal rotation by means of electron diffraction. Ferrocene and ruthenocene, *Acta Chem. Scand.* 22 (1968) 2653–2670.
- [25] G. Clech, G. Calvarin, J.F. Berar, R. Kahn, Ferrocene $Fe(C_5H_5)_2$ ordered and disordered structural phases, *Comptes Rendus des Seances de l'Academie des Sciences Serie C* 286 (1978) 315–317.
- [26] G. Clech, G. Calvarin, J.F. Berar, D. Andre, Determination of the molecular configuration of ferrocene $[Fe(C_5H_5)_2]$ in the ordered phase at 130 K, *Comptes Rendus des Seances de l'Academie des Sciences Serie C* 287 (1978) 523–525.
- [27] F. Takusagawa, T.F. Koetzle, A neutron diffraction study of the crystal structure of ferrocene, *Acta Crystallogr. B* B35 (1979) 1074–1081.
- [28] M. Appel, B. Frick, T.L. Spehr, B. Stühn, Molecular ring rotation in solid ferrocene revisited, *J. Chem. Phys.* 142 (2015) 114503.
- [29] M. Bühl, S. Grigoleit, Molecular dynamics of neutral and protonated ferrocene#, *Organometallics* 24 (2005) 1516–1527.
- [30] J.N. Canongia Lopez, P. do Couto, M.E. da Piedade, An all-atom force field for metallocenes, *J. Phys. Chem. A* 110 (2006) 13850–13856.
- [31] M.T. Islam, S.P. Best, J.D. Bourke, L.J. Tantau, C.Q. Tran, F. Wang, C.T. Chantler, Accurate X-ray absorption spectra of dilute systems: absolute measurements and structural analysis of ferrocene and decamethylferrocene, *J. Phys. Chem. C* 120 (2016) 9399–9418.
- [32] J.D. Bourke, M.T. Islam, S.P. Best, C.Q. Tran, F. Wang, C.T. Chantler, Conformation analysis of ferrocene and decamethylferrocene via full-potential modeling of XANES and XAFS spectra, *J. Phys. Chem. Lett.* 7 (2016) 2792–2796.
- [33] S. Coriani, A. Haaland, T. Helgaker, P. Jørgensen, The equilibrium structure of ferrocene, *ChemPhysChem* 7 (2006) 245–249.
- [34] T.P. Gryaznova, S.A. Katsyuba, V.A. Milyukov, O.G. Sinyashin, DFT study of substitution effect on the geometry, IR spectra, spin state and energetic stability of the ferrocenes and their pentaphospholyl analogues, *J. Organomet. Chem.* 695 (2010) 2586–2595.
- [35] D.E. Bean, P.W. Fowler, M.J. Morris, Aromaticity and ring currents in ferrocene and two isomeric sandwich complexes, *J. Organomet. Chem.* 696 (2011) 2093–2100.
- [36] D.R. Roy, S. Duley, P.K. Chattaraj, Bonding, reactivity and aromaticity in some novel all-metal metallocenes, *Proc. Ind. Natl. Sci. Acad.* 74 (2008) 11.
- [37] Y. Yamaguchi, W. Ding, C.T. Sanderson, M.L. Borden, M.J. Morgan, C. Kutal, Electronic structure, spectroscopy, and photochemistry of group 8 metallocenes, *Coord. Chem. Rev.* 251 (2007) 515–524.
- [38] J.S. Bodenheimer, W. Low, A vibrational study of ferrocene and ruthenocene, *Spectrochim. Acta Part A: Mol. Spectroscopy* 29 (1973) 1733–1743.
- [39] P.A. Silva, T.M.R. Maria, C.M. Nunes, M.E.S. Eusébio, R. Fausto, Intermolecularly-induced conformational disorder in ferrocene, 1-bromoferrocene and 1,1-di-bromoferrocene, *J. Mol. Struct.* 1078 (2014) 90–105.
- [40] K. Chhor, G. Lucazeau, C. Sourisseau, Vibrational study of the dynamic disorder in nickelocene and ferrocene crystals, *J. Raman Spectrosc.* 11 (1981) 183–198.
- [41] P. Seiler, J.D. Dunitz, Low-temperature crystallization of orthorhombic ferrocene: structure analysis at 98 K, *Acta Crystallogr. Section B: Struct. Crystallogr. Cryst. Chem.* 38 (1982) 1741–1745.
- [42] A.J. Campbell, C.A. Pyfe, D. Harold-smith, K.R. Jeffrey, An investigation of the dynamic structures of ferrocene, ruthenocene and dibenzenechromium in the solid state and in solution, *Mol. Cryst. Liq. Cryst.* 36 (1976) 1–23.
- [43] J.A. Ruiz-Santoyo, M. Rodríguez-Matus, J.L. Cabellos, J.T. Yi, D.W. Pratt, M. Schmitt, G. Merino, L. Álvarez-Valtierra, Intramolecular structure and dynamics of mequinol and guaicol in the gas phase: rotationally resolved electronic spectra of their S1 states, *J. Chem. Phys.* 143 (2015) 094301.
- [44] R.K. Bohn, A. Haaland, On the molecular structure of ferrocene, *J. Organomet. Chem.* 5 (1966) 470–476.
- [45] L.G. Domracheva, N.V. Karyakin, M.S. Sheiman, G.V. Kamelova, V.N. Larina, O.N. Suvarova, G.A. Domrachev, Thermodynamics and molecular dynamics of some ferrocene derivatives, *Russ. Chem. Bull.* 48 (1999) 1647–1655.
- [46] E.A. Seibold, L.E. Sutton, Structure of ferrocene, *J. Chem. Phys.* 1955 (1967) 23.
- [47] A. Kubo, R. Ikeda, D. Nakamura, Motion of C5H5 rings in three crystalline modifications of ferrocene as studied by 1H NMR, *Chem. Lett.* (1981) 1497–1500.
- [48] N. Mohammadi, F. Wang, S.P. Best, D. Appadoo, C.T. Chantler, Dominance of eclipsed ferrocene conformer in solutions revealed by the IR fingerprint spectral splitting. [arXiv:1306.0633](https://arxiv.org/abs/1306.0633), 2013.
- [49] J.D. Dunitz, Phase changes and chemical reactions in molecular crystals, *Acta Crystallogr. Section B Struct. Sci.* 51 (1995) 619–631.
- [50] C.H. Holm, J.A. Ibers, NMR study of ferrocene, ruthenocene, and titanocene dichloride, *J. Chem. Phys.* 30 (1959) 885–888.
- [51] P. Seiler, J.D. Dunitz, A new interpretation of the disordered crystal structure of ferrocene, *Acta Crystallogr. Section B Struct. Crystallogr. Cryst. Chem.* 35 (1979) 1068–1074.